Available online at www.sciencedirect.com
ScienceDirect
Journal of Power Sources 159 (2006) 1353–1359
JOURNAL OF POWER SOURCES
www.elsevier.com/locate/jpowsour

The preparation and electrochemical performance of solid solutions $LiCoO_2$–Li_2MnO_3 as cathode materials for lithium ion batteries

Yucheng Sun [a,b], Yuki Shiosaki [b], Yonggao Xia [b], Hideyuki Noguchi [b,*]

[a] *Venture Business Laboratory, Saga University, Honjo-1, Saga 840-8520, Japan*
[b] *Department of Applied Chemistry, Saga University, Honjo-1, Saga 840-8520, Japan*

Received 18 October 2005; received in revised form 8 December 2005; accepted 8 December 2005
Available online 24 January 2006

Abstract

In the paper, we have investigated the preparation and electrochemical performance of the solid solution Li_2MnO_3–$LiCoO_2$ (or written as $Li[Li_{x/3}Co_{1-x}Mn_{2x/3}]O_2$). The chemical composition determined by ICP–AES indicates that the chemical formula of our prepared samples is very closely to that of the ideal Li_2MnO_3–$LiCoO_2$ solid solution in chemical stoichiometry. It was found that the oxidation states of Co and Mn are +3 and +4, respectively by redox titration and X-ray photoelectron spectroscopy (XPS). XRD shows that most peaks of the samples prepared at 950 °C could be simply indexed as a layered α-$NaFeO_2$ structure (space group $R\bar{3}m$, no. 166) except some additional peaks between 21° and 25°, which is caused by the appearance of the superlattice structure. The monoclinic phase has been formed for $Li[Li_{x/3}Co_{1-x}Mn_{2x/3}]O_2$ ($x = 0.5$) at 750 °C, which is reversibly transformed into a hexagonal phase with the increasing of sintering temperature from 750 to 950 °C. It is found that the charge capacity of the samples $Li[Li_{x/3}Co_{1-x}Mn_{2x/3}]O_2$ ($0.5 \leq x \leq 0.7$) increases and the discharge capacity has no obvious change with the increasing of the sintering temperature due to the appearance of a flat charge voltage plateau at 4.45 V. Moreover, the discharge capacity of the samples gradually reduces with the increasing Li_2MnO_3 content. The sample has the excellent electrochemical cycling performance with the charge–end voltage of 4.5 V. XRD patterns of the charged product indicate that the layered structure has been kept during the charge process, which may be the reason for its good cycling performance.

Keywords: Lithium-ion batteries; Cathode materials; Solid solutions; Cycling performance; $LiCoO_2$–Li_2MnO_3

1. Introduction

Until now many compounds [1–7] have been extensively studied as the single transition-metal cathode materials, such as $LiCoO_2$, $LiNiO_2$, $LiMn_2O_4$, $LiFePO_4$ and $LiMnO_2$. Although these materials have their own advantages, their disadvantages are also evident, such as higher cost of $LiCoO_2$, the poor thermal stability of $LiNiO_2$ and the capacity fading of $LiMn_2O_4$ at elevated temperature. Recently, there has been a growing interest in complicated compositional cathode materials for advanced lithium ion batteries. $LiNi_{1-x}Co_xO_2$ [8–10] has been studied as the earliest complicated cathode material, which can be regarded as the solid solution of $LiCoO_2$ and $LiNiO_2$. Compared with $LiCoO_2$ and $LiNiO_2$, $LiNi_{1-x}Co_xO_2$ has not only retained the high capacity but also improved the cycling performance and thermal stability while it reduces the material cost due to the less content of the expensive Co. In order to further improve the structural and thermal stability, a series of Li–Ni–Co–Mn–O compounds [11–19] have been prepared and their physical and electrochemical properties have been extensively studied. These compounds can be regarded as the solid solution of $LiNiO_2$, Li_2MnO_3 (or $LiMnO_2$) and $LiCoO_2$. The complicated compounds have retained the advantages of its single transition-metal species and overcome their shortcomings, which has extended the research fields of the cathode materials for lithium ion batteries. Recently, many solid solution systems have been widely studied such as $LiCrO_2$–Li_2MnO_3 [20–23], $LiNiO_2$–Li_2MnO_3 [12,24–26], $LiNiO_2$–Li_2MnO_3–$LiCoO_2$ [14], $LiNi_{0.5}Mn_{0.5}O_2$–Li_2MnO_3 [27], Li_2MnO_3–$LiNi_{1-x}Co_xO_2$ [28], Li_2MnO_3–$LiCoO_2$ [29,30], $LiNi_{0.5}Mn_{0.5}O_2$–Li_2MnO_3–$LiCoO_2$ [31], $LiFeO_2$–Li_2MnO_3 [32,33], $LiNi_{0.5}Mn_{0.5}O_2$–Li_2TiO_3 [34,35], $LiCrO_2$–

* Corresponding author. Tel.: +81 952 28 8674; fax: +81 952 28 8591.
E-mail address: noguchih@cc.saga-u.ac.jp (H. Noguchi).

0378-7753/$ – see front matter © 2006 Elsevier B.V. All rights reserved.
doi:10.1016/j.jpowsour.2005.12.037

Li_2TiO_3 [36,37] and $LiNiO_2$–Li_2TiO_3 [38,39]. Therefore, it is possible to discover some promising cathode materials for lithium ion batteries by studying these different solid solutions.

In this paper, the preparation, the structure and electrochemical performance of solid solution Li_2MnO_3–$LiCoO_2$ have been studied. It has been focused on the effects of sintering temperature and composition change on the structure and the reversible capacity of the samples. Moreover, we have determined the average valence of Co and Mn by chemical analysis and found that the structure of solid solution $Li[Li_{x/3}Co_{1-x}Mn_{2x/3}]O_2$ ($x = 0.5$) can reversibly transform between a monoclinic phase and a hexagonal phase in the temperature ranges of 750–950 °C.

2. Experimental

The samples were prepared by the following process. The desired amount of $LiCH_3COO{\cdot}2H_2O$, $Co(CH_3COO)_2{\cdot}4H_2O$ and $Mn(CH_3COO)_2{\cdot}4H_2O$ were dissolved in water with the aid of citric acid. The transparent solution was fed into a spray drying instrument (pulvis mini-spray GB22, Yamato, Japan) to produce a homogenous precursor. The excess Li salt was added in the preparation process of the precursor. The precursor was initially decomposed at 400 °C in air and then ground after cooling. The decomposed mixture was calcined at 750–950 °C in air for 15 h. The prepared samples were dispersed into distilled water and excess lithium was washed out. The desired sample was filtered out and was calcined again for 1 h at the same sintering temperature.

The chemical composition of Li, Co and Mn was measured by inductively coupled plasma–atomic emission spectroscopy (ICP–AES) and are listed Table 1. The average valence of Mn and Co was determined by the redox titration method using $KMnO_4$ as an oxidized reagent [40]. Powder X-ray diffraction (XRD, Rint-1000, Rigaku, Japan) measurement using Cu Kα radiation was employed to identify the crystalline phase of the synthesized material. XRD data ($2\theta = 10$–$80°$) had a step size of 0.02°. Lattice parameters were calculated directly by the least squares refinement based on a hexagonal unit cell. X-ray photoelectron spectroscopy (XPS) measurements were carried out using a Kratos XSAM 800 spectrometer with Al Kα radiation. The binding energy was calibrated with respect to the conductive C 1 s (285.0 eV).

The charge–discharge tests were carried out using a CR2032 coin-type cell, which consists of a cathode and lithium metal anode separated by a Celgard 2400 porous polypropylene film. The electrolyte solution was 1 M $LiPF_6$ in a mixture of ethylene carbonate (EC) and dimethyl carbonate (DMC) in a 1:1 volume ratio. The cathodes were prepared by blending 20 mg active materials and 12 mg the conducting binder of teflonized acetylene black (TAB 2). The mixture was pressed onto a nickel screen and dried at 170 °C for 5 h in a vacuum state. The cell was assembled in an argon-filled glove box and tested using a constant charge–discharge current density of 0.4 mA cm^{-2}. The cells were typically cycled in the voltage ranges of 3.0–4.5 V, 3.0–4.6 V, 3.0–4.7 V and 3.0–4.8 V at room temperature or elevated temperature.

Table 1
Composition, the content of Li, Co and Mn, the average oxidation of Co and Mn for the samples

Chemical formula	Mole ratio			Average valence
	Li	Co	Mn	
$Li_{1.16}Co_{0.42}Mn_{0.43}O_{2.06}$				
Mesu.	1.21	0.577	0.377	3.39
Cal.	1.23	0.585	0.382	3.39
$Li_{1.16}Co_{0.42}Mn_{0.43}O_{2.06}$				
Mesu.	1.28	0.465	0.472	3.52
Cal.	1.30	0.470	0.478	3.50
$Li_{1.19}Co_{0.33}Mn_{0.43}O_{2.05}$				
Mesu.	1.35	0.368	0.547	3.60
Cal.	1.37	0.375	0.556	3.60
$Li_{1.23}Co_{0.24}Mn_{0.54}O_{2.03}$				
Mesu.	1.44	0.278	0.628	3.66
Cal.	1.45	0.281	0.635	3.69
$Li_{1.25}Co_{0.15}Mn_{0.60}O_{2.04}$				
Mesu.	1.48	0.181	0.710	3.77
Cal.	1.50	0.184	0.719	3.80
$Li_{1.28}Co_{0.07}Mn_{0.65}O_{2.06}$				
Mesu.	1.53	0.087	0.778	3.93
Cal.	1.56	0.089	0.794	3.90

3. Results and discussion

Six solid solution Li_2MnO_3–$LiCoO_2$ samples (alternatively in layered notation $Li[Li_{x/3}Co_{1-x}Mn_{2x/3}]O_2$) have been selected for consideration, namely $x = 0.5$, 0.6, 0.69, 0.78, 0.86 and 0.93. Table 1 shows the content of Li, Co and Mn, which was measured by ICP and the average oxidation of Co and Mn determined by a combination of the data of a redox titration and the content of the transition metal elements. It has been found that the measured average valence values are basically consistent with the calculated values based on the combination of Co^{3+} and Mn^{4+}. Therefore, it is believed that Co and Mn in our prepared samples present +3 and +4, respectively. The O content could be calculated from the content of metal cations and their oxidation states. The measured results of the elements Li, Mn and Co by inductively coupled plasma–atomic emission spectroscopy indicated that the chemical formula of our prepared samples is very closely to the ideal Li_2MnO_3–$LiCoO_2$ chemical stoichiometry, although there is a small amount of excess oxygen.

Fig. 1 indicates Co 2P and Mn 2P XPS spectra of $Li[Li_{x/3}Co_{1-x}Mn_{2x/3}]O_2$ with $x = 0.6$ and $LiNi_{1/3}Co_{1/3}Mn_{1/3}O_2$. It was found that the binding energy of Mn $2P_{3/2}$ is 642.3 eV, which is very close to that (642.4 eV) of Mn $2P_{3/2}$ in λ-MnO_2. So it is believed that the valence state of Mn in the sample is +4. Moreover, the Co 2P and Mn 2P spectra of $Li[Li_{0.2}Co_{0.4}Mn_{0.4}]O_2$ is almost the same as that of $LiNi_{1/3}Co_{1/3}Mn_{1/3}O_2$, in which the valence state of Co and Mn is confirmed to be +3 and +4, respectively [41]. Therefore, it is assured that the valence states of Co and Mn in $Li[Li_{0.2}Co_{0.4}Mn_{0.4}]O_2$ are +3 and +4, respectively, which is well consistent with the measured results of a redox titration.

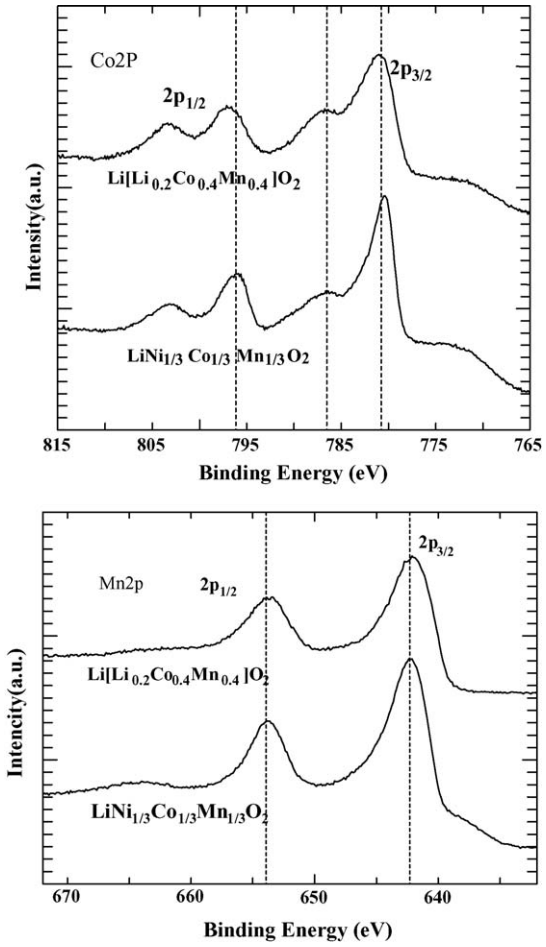

Fig. 1. Co 2p and Mn 2p XPS spectra of $Li[Li_{x/3}Co_{1-x}Mn_{2x/3}]O_2$ with $x = 0.6$ and $LiNi_{1/3}Co_{1/3}Mn_{1/3}O_2$.

Fig. 2 showed the XRD patterns of the six solid solutions $Li[Li_{x/3}Co_{1-x}Mn_{2x/3}]O_2$ prepared at 950 °C. Most of peaks could be simply indexed as a layered α-$NaFeO_2$ structure (space group $R\bar{3}m$, no. 166). There are some sawtooth peaks between

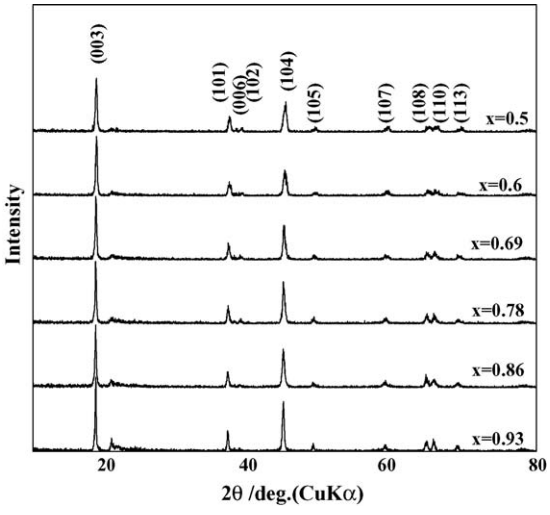

Fig. 2. XRD patterns of the six solid solutions $Li[Li_{x/3}Co_{1-x}Mn_{2x/3}]O_2$ prepared at 950 °C.

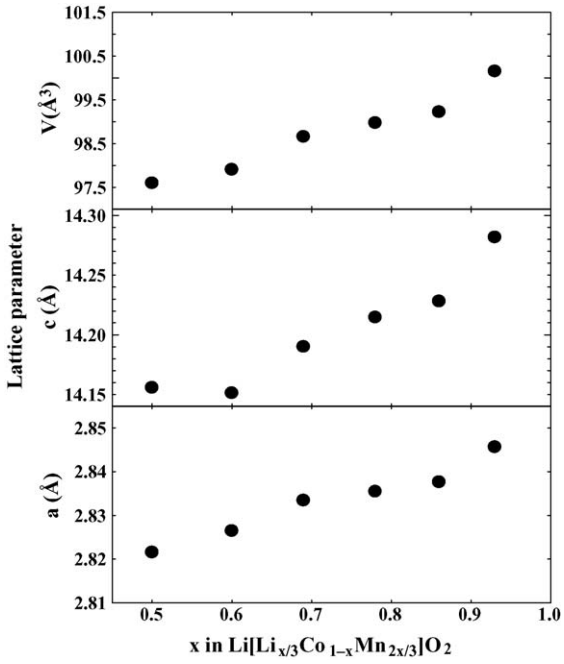

Fig. 3. The change in lattice parameters a, c and unit cell volume for solid solutions $Li[Li_{x/3}Co_{1-x}Mn_{2x/3}]O_2$.

21° and 25°, which are caused by the superlattice structure of Li_2MnO_3. The crystal structure of Li_2MnO_3 consists of cubic closed-packed oxide ion layers with alternate sheets of octahedral sites occupied by Li and $[Li_{1/3}Mn_{2/3}]$ and shows a 1:2 cation order of Li and Mn in $[Li_{1/3}Mn_{2/3}]$, resulting in the space group $C_{2/m}$ [42,43]. If the Li and Mn ions in $[Li_{1/3}Mn_{2/3}]$ layers are randomly distributed, the crystal structure of Li_2MnO_3 is the same as that of O_3–$LiCoO_2$ with space group $R\bar{3}m$. The superlattice peaks become broad as the $[Li_{1/3}Mn_{2/3}]$ is partly replaced by Co^{3+} because the 1:2 stoichiometry of Li and Mn ions is destroyed and the charge difference between Li^+ and Co^{3+} is less than that between Li^+ and Mn^{4+}. The lattice parameters of the samples were calculated using the related pseudo-hexagonal $R\bar{3}m$ type unit cell, as shown in Fig. 3. With the increases of x in $Li[Li_{x/3}Co_{1-x}Mn_{2x/3}]O_2$, the lattice parameters a and c have linearly increased, which indicates that a true solid solution is formed in this composition range. Moreover, the cell volume of the solid solution $Li[Li_{x/3}Co_{1-x}Mn_{2x/3}]O_2$ increases from 97.5 Å^3 for $x = 0.5$–100.16 Å^3 for $x = 0.93$. Because the ionic radius of Li^+ (0.76 Å) is lager than that of Co^{3+} (0.63 Å), the cell volume will increase with the increasing of Li^+ content in $[Li_{x/3}Co_{1-x}Mn_{2x/3}]$ layers.

We have also studied the effects of sintering temperature on the structure of solid solution $Li[Li_{0.2}Co_{0.4}Mn_{0.4}]O_2$. Fig. 4 indicated the XRD patterns of the sample $Li[Li_{0.2}Co_{0.4}Mn_{0.4}]O_2$ at various temperatures. Firstly, main characteristic peaks of a layered structure can be found from the samples prepared at 750–950 °C. However, the sample prepared at 750 °C would have a monoclinic phase, in which the splits of both (1 0 1) and (1 0 4) peaks are observed. With the increasing of the sintering temperature from 750 to 950 °C, the shoulder peaks of (1 0 1) and (1 0 4) disappear and the splits in the (0 0 6)/(0 1 2)

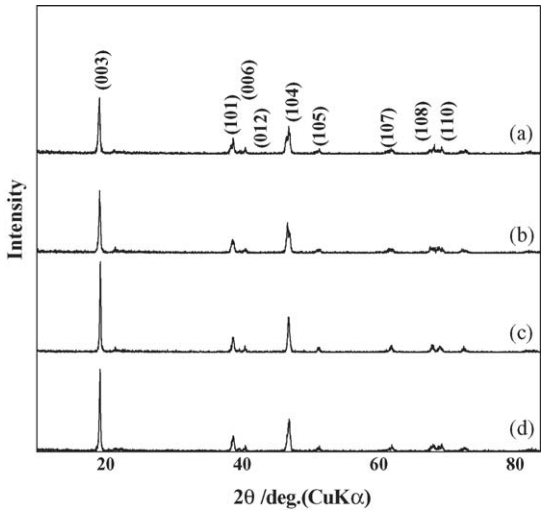

Fig. 4. XRD patterns of the samples $Li[Li_{x/3}Co_{1-x}Mn_{2x/3}]O_2$ at (a) 750 °C; (b) 850 °C; (c) 950 °C; (d) sintered at 950 °C and then slowly cooled down to 750 °C.

and (1 0 8)/(1 1 0) doublets become more and more sharp, which means that a phase transformation happened from a monoclinic phase to a hexagonal phase structure. The sample prepared at 950 °C has a hexagonal phase structure, although there are still some weak peaks between 21° and 25°, which are caused by the superlattice structure as in Li_2MnO_3. Fig. 4(d) shows the XRD patterns of the sample, which is initially sintered at 950 °C and then slowly cooled down to 750 °C. It was found that it has a monoclinic phase, the same as that of the sample prepared at 750 °C, which means that a reversible phase structure transformation occurred at 750–950 °C.

Fig. 5 shows the charge–discharge curves of $Li[Li_{x/3}Co_{1-x}Mn_{2x/3}]O_2$ ($0.5 \le x \le 0.78$) prepared at different sintering temperature. It was found that the sintering temperature has the important effects on the electrochemical performance of the samples. The sample prepared at 950 °C has two charge plateaus at its first charge curves as for $0.5 \le x \le 0.69$, which is obviously different from that of the samples prepared at 750 °C. The first charge and discharge irreversible capacity of $Li[Li_{x/3}Co_{1-x}Mn_{2x/3}]O_2$ with $x = 0.6$ increases from 16.5 mAh g^{-1} at 750 °C to 59.3 mAh g^{-1} at 950 °C due to the appearance of the flat charge voltage plateau at 4.45 V for the sample prepared at 950 °C, which is not the corresponding discharge voltage plateau. It was found that the flat charge plateau at 4.45 V become shorter and shorter with the increasing of Mn content and disappears at the second charge curve. With the increasing of Mn content, the charge–discharge capacity of the sample has gradually decreased and the effects of sintering temperature on its charge–discharge curves have become no more obvious.

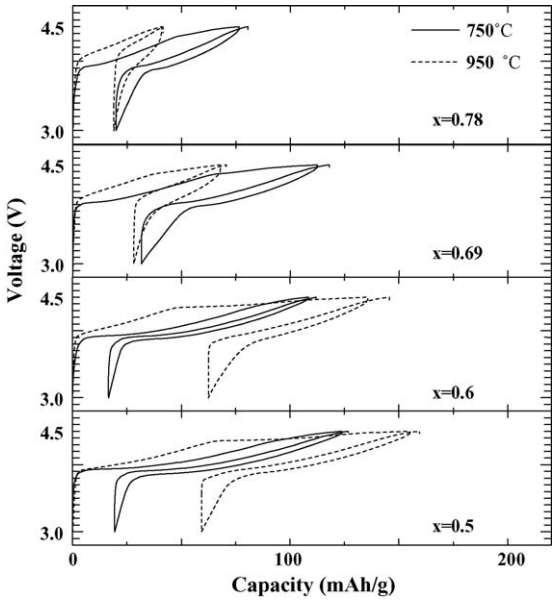

Fig. 5. The charge–discharge curves of $Li[Li_{x/3}Co_{1-x}Mn_{2x/3}]O_2$ ($0.5 \le x \le 0.78$) prepared at different sintering temperatures.

Fig. 6 indicates the theoretical capacity and the reversible capacity of the samples $Li[Li_{x/3}Co_{1-x}Mn_{2x/3}]O_2$ ($0.5 \le x \le 0.93$) in the voltage range of 3.0–4.5 V. The theoretical discharge capacity can be calculated based on the Co^{3+} oxidation and Co^{4+} reduction during the charge and discharge process. It is found that the discharge capacity of both samples prepared at 750 and at 950 °C gradually decreases with the improvement of Mn content, which is consistent with the change of the theoretical capacity. When $x \ge 0.69$, the samples prepared at 750 °C have the higher discharge capacity. But when $x \le 0.69$, the samples prepared at 950 °C have the higher discharge capacity than that of the samples prepared at lower 750 °C. It means that the samples with less Mn content should be prepared at higher sintering temperature and the samples with more Mn content should be prepared at lower sintering temperature in order to obtain the better electrochemical performance of the samples.

We have further studied the effects of the charge–end voltage on the electrochemical performance of $Li[Li_{x/3}Co_{1-x}Mn_{2x/3}]O_2$ with $x = 0.6$ prepared at 750 °C. Fig. 7 shows the charge and discharge curves of the samples $Li[Li_{x/3}Co_{1-x}Mn_{2x/3}]O_2$ with $x = 0.6$ in the voltage ranges of 3.0–4.5 V, 3.0–4.6 V, 3.0–4.7 V and 3.0–4.8 V. With the improvement of the charge–end voltage, the charge capacity of the sample gradually increases from 200 mAh g^{-1} for 4.6 V charge–end voltage to 252.8 mAh g^{-1} for 4.8 V charge–end voltage, but the discharge capacity does

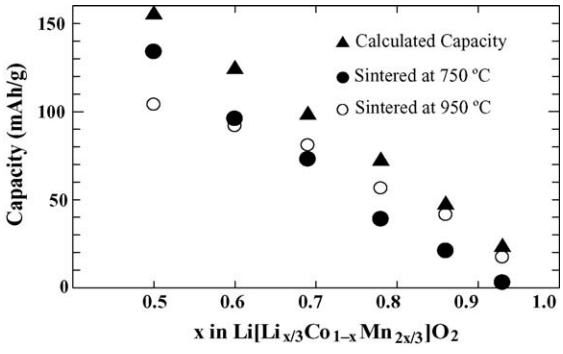

Fig. 6. The theoretical discharge capacity and the measured reversible capacity of the samples $Li[Li_{x/3}Co_{1-x}Mn_{2x/3}]O_2$ prepared at different temperatures.

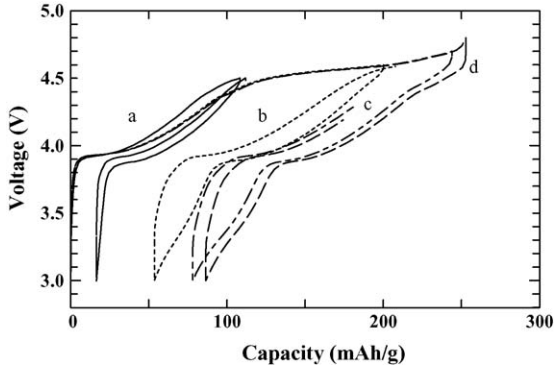

Fig. 7. The charge and discharge curves of the samples $Li[Li_{x/3}Co_{1-x}Mn_{2x/3}]O_2$ with $x = 0.6$ and the charge voltage voltages between (a) 3.0–4.5 V; (b) 3.0–4.6 V; (c) 3.0–4.7 V and (d) 3.0–4.8 V.

not increase after the charge–end voltage attains to 4.7 V. The sample has the almost same as discharge capacities at 4.7 V charge–end voltage (165.8 mAh g^{-1}) and 4.8 V charge–end voltage (166.4 mAh g^{-1}). A long flat voltage plateau at about 4.6 V appears and the charge capacity is far higher than the theoretical capacity based on the Co^{3+} oxidation and Co^{4+} reduction during the charge and discharge process, which could be found at 4.45 V for the sample prepared at 950 °C, as shown in Fig. 5. It is believed that the flat high voltage plateau should be ascribed to the removal of Li_2O [27] from solid solution $LiCoO_2$–Li_2MnO_3.

Fig. 8 shows the charge and discharge curves of $Li[Li_{x/3}Co_{1-x}Mn_{2x/3}]O_2$ ($x = 0.6$) at elevated temperature (60 °C) in the voltage range of 3.0–4.5 V, which is prepared at 750 °C. Compared with the data at room temperature, the charge capacity attains to 196.5 mAh g^{-1}, which is higher than the theoretical capacity based on the Co^{3+} oxidation and Co^{4+} reduction during the charge and discharge process. The first irreversible capacity is 71.8 mAh g^{-1}, far higher than that of the sample measured at room temperature (16.2 mAh g^{-1}). There is a high charge–voltage plateau corresponding to the irreversible capacity, which is not found at room temperature when it is charged to 4.5 V. Therefore, it indicated that the electrode polarization becomes smaller and the flat high voltage plateau appears at lower charge–voltage when it is measured at elevated temperature, which shows that the removal of Li_2O from solid solution $LiCoO_2$–Li_2MnO_3 would be controlled by the kinetic factor.

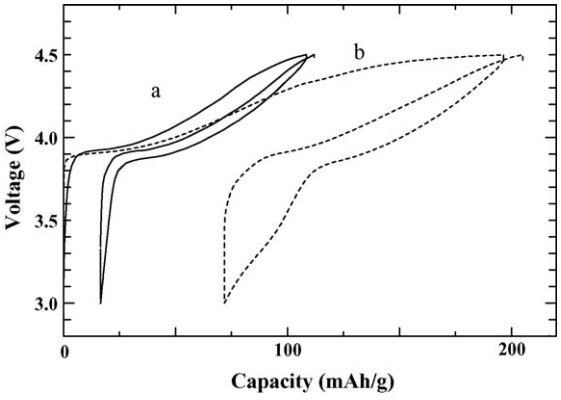

Fig. 8. The charge and discharge curves of $Li[Li_{x/3}Co_{1-x}Mn_{2x/3}]O_2$ ($x = 0.6$) prepared at 750 °C, which was measured at (a) room temperature and (b) elevated temperature (60 °C) in the voltage ranges of 3.0–4.5 V.

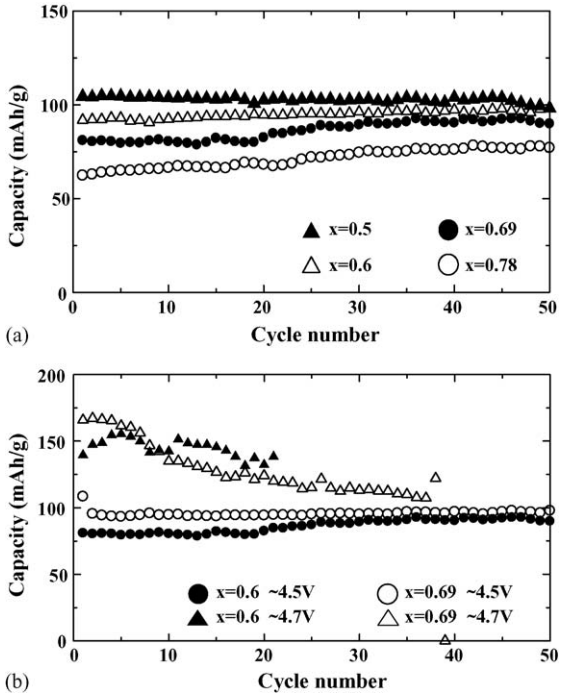

Fig. 9. The electrochemical cycling performance of $Li[Li_{x/3}Co_{1-x}Mn_{2x/3}]O_2$ with various x values and in the various charge–discharge voltage ranges.

The electrochemical cycling performance of $Li[Li_{x/3}Co_{1-x}Mn_{2x/3}]O_2$ with various x values is indicated in Fig. 9. The sample has the excellent electrochemical cycling performance in the voltage range of 3.0–4.5 V. For $Li[Li_{x/3}Co_{1-x}Mn_{2x/3}]O_2$, with $x = 0.6$, the discharge capacity of the sample is 100 mAh g^{-1} and the capacity retention is almost 100% after 50 cycles. Compared with $LiCoO_2$, the cycling performance of the samples have been greatly improved by forming the solid solution $Li[Li_{x/3}Co_{1-x}Mn_{2x/3}]O_2$ even charged to 4.5 V, although the reversible capacity has a decrease. Moreover, the reversible capacity of the samples gradually decreases with the increasing of Li_2MnO_3. Fig. 9(b) shows that the cycling performance of the sample becomes poor with the further increasing of the charge–end voltage. For example, the discharge capacity of $Li[Li_{x/3}Co_{1-x}Mn_{2x/3}]O_2$ with $x = 0.6$ decreases from 160 mAh g^{-1} of the initial discharge capacity to 120 mAh g^{-1} of the 35th cycle and the capacity retention has only 75% after 35 cycles when it is charged up to 4.7 V. It is believed that the poor cycling performance of the sample at the charge–end voltage above 4.5 V is related with the appearance of a long high voltage plateau, which is corresponding to the removal of Li_2O from solid solution $LiCoO_2$–Li_2MnO_3. Therefore, the charge–end voltage of the solid solutions should be restricted at 4.5 V. For $Li[Li_{x/3}Co_{1-x}Mn_{2x/3}]O_2$ with $x = 0.69$, 0.78, 0.86 and 0.93, the same excellent cycling performance has been found in the voltage ranges of 3.0–4.5 V, although the reversible capacity decreases with the increasing of x value.

XRD was used to investigate the structural change of the sample during the electrochemical lithium de-insertion

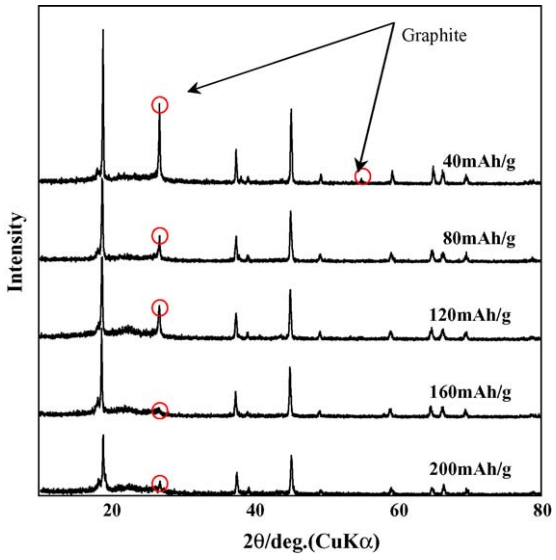

Fig. 10. XRD patterns of the sample $Li[Li_{x/3}Co_{1-x}Mn_{2x/3}]O_2$ with $x = 0.6$ during the different lithium extraction stages.

process. Fig. 10 shows the XRD patterns of the sample $Li[Li_{x/3}Co_{1-x}Mn_{2x/3}]O_2$ with $x = 0.6$ during the different lithium extraction stages. It is found that no structural changes have occurred even the charge capacity attains to 200 mAh g^{-1} and the layered structure has always kept, which is different from $LiCoO_2$ [44,45]. It may be the reason why it has the excellent cycling performance for the solid solution $LiCoO_2$–Li_2MnO_3 even charged to 4.5 V.

4. Conclusions

Solid solutions $LiCoO_2$–Li_2MnO_3 have been successfully prepared by a spray drying method between 750 and 950 °C. XRD shows that most peaks of the samples prepared at 950 °C could be simply indexed as a layered α-$NaFeO_2$ structure (space group $R\bar{3}m$, no. 166) except that some sawtooth peaks between 21° and 25°, which are caused by the superlattice structure as Li_2MnO_3. With the increasing of the sintering temperature from 750 to 950 °C, a long flat charge plateau at 4.45 V appears, which causes the large irreversible capacity. It is believed that the charge capacity at the flat high charge plateau is caused by the Li_2O removal from solid solutions $LiCoO_2$–Li_2MnO_3. Electrochemical measurements showed that the discharge capacity of the samples gradually reduces with the increasing of Li_2MnO_3 content and the excellent electrochemical cycling performance can be obtained when it is charged to 4.5 V. It indicated that the layered structure of the sample has been always kept until the charge capacity attain to 200 mAh g^{-1}, which may be the reason for its excellent cycling performance.

Acknowledgement

This work was partly supported by the Venture Business Laboratory of Saga University.

References

[1] K. Mizushima, P.C. Jones, J.B. Goodenough, Mater. Res. Bull. 15 (1980) 783.
[2] M.M. Thackeray, W.I.F. David, P.G. Bruce, J.B. Goodenough, Mater. Res. Bull. 18 (1983) 461.
[3] M.G.S.R. Thomas, W.I.F. David, J.B. Goodenough, Mater. Res. Bull. 20 (1985) 1137.
[4] A.R. Armstrong, P.G. Bruce, Nature 499 (1996) 138.
[5] A.R. Armstrong, P.G. Bruce, Nature 499 (1996) 381.
[6] H. Tukamoto, A.R. West, J. Electrochem. Soc. 144 (1997) 3164.
[7] A.K. Padhi, K.S. Nanjundaswamy, J.B. Goodenough, J. Electrochem. Soc. 144 (1997) 1188.
[8] A. Lecerf, M. Broussely, J.P. Gabano, EP patent no. 0345707, US patent no. 4980080 (1989).
[9] T. Ohzuku, H. Komori, K. Sawai, T. Hirai, Chem. Express 5 (1990) 733.
[10] M. Balasubramanian, X. Sun, X.Q. Yang, J. McBreen, J. Electrochem. Soc. 147 (2000) 2903.
[11] T. Ohzuku, Y. Makimura, Chem. Lett. (2001) 744.
[12] Z. Lu, D.D. MacNeil, J.R. Dahn, Electrochem. Solid-State Lett. 4 (2001) A191.
[13] T. Ohzuku, Y. Makimura, Chem. Lett. (2001) 642.
[14] Y. Sun, C. Ouyang, Z. Wang, X. Huang, L. Chen, J. Electrochem. Soc. 151 (2004) A504.
[15] Y. Makimara, T. Ohzuku, J. Power Sources 119–121 (2003) 156.
[16] S.-H. Kang, K. Amine, J. Power Sources 119–121 (2003) 150.
[17] N. Yabuuchi, T. Ohzuku, J. Power Sources 119–121 (2003) 171.
[18] S. Jouanneau, K.W. Eberman, L.J. Krause, J.R. Dahn, J. Electrochem. Soc. 150 (2003) 1637.
[19] D.-C. Li, H. Noguchi, M. Yoshio, Electrochim. Acta 50 (2004) 427.
[20] B. Ammundsen, J. Desilvestro, R. Steiner, P. Pichering, in: Proceedings of the 10th International Meeting on Lithium Batteries, Como, Italy, 28 May–2 June, 2000 (Abstract no. 17).
[21] C. Storey, I. Kargina, Y. Grincourt, I.J. Davidson, Y.C. Yoo, D.Y. Seung, J. Power Sources 97–98 (2001) 541.
[22] M. Balasubramanian, J. Mcbreen, I.J. Davidson, P.S. Whitfield, I. Kargina, J. Electrochem. Soc. 149 (2002) A176.
[23] Z. Lu, J.R. Dahn, J. Electrochem. Soc. 149 (2002) A1454.
[24] L. Zhang, H. Noguchi, M. Yoshio, J. Power Sources 110 (2002) 57.
[25] Z. Lu, J.R. Dahn, J. Electrochem. Soc. 149 (2002) A778.
[26] S.-S. Shin, Y.-K. Sun, K. Amine, J. Power Sources 112 (2002) 634.
[27] C.S. Johnson, J.-S. Kim, C. Lefief, N. Li, J.T. Vaughey, M.M. Thackeray, Electrochem. Commun. 6 (2004) 1085.
[28] P.S. Whitfield, S. Niketic, I.J. Davidson, J. Power Sources 146 (2005) 617.
[29] P.S. Whitfield, S.Argue, I.J. Davidson, in: Second Lithium Battery Discussion, Arcachon, France, 15–19 September, 2003 (Abstract no. 59).
[30] K. Numata, C. Sakaki, S. Yamanaka, Solid State Ionics 117 (1999) 257.
[31] L. Zhang, K. Takada, N. Ohta, K. Fukuda, T. Sasaki, J. Power Sources 146 (2005) 598.
[32] M. Tabuchi, H. Shigemura, K. Ado, H. Kobayashi, H. Sakaebe, H. Kageyama, R. Kanno, J. Power Sources 97–98 (2001) 415.
[33] M. Tabuchi, A. Nakashima, H. Shigemura, K. Ado, H. Kobayashi, H. Sakaebe, H. Kageyama, T. Nakamura, H. Kohzaki, A. Hirano, R. Kanno, J. Electrochem. Soc. 149 (2002) A509.
[34] J.S. Kim, C.S. Johnson, M.M. Thackeray, Electrochem. Commun. 4 (2002) 205.
[35] C.S. Johnson, J.S. Kim, A.J. Kropf, A.J. Kahaian, J.T. Vaughey, M.M. Thackeray, Electrochem. Commun. 4 (2002) 492.
[36] L. Zhang, H. Noguchi, Electrochem. Commun. 4 (2002) 560.
[37] L. Zhang, H. Noguchi, J. Electrochem. Soc. 150 (2003) A607.
[38] L. Zhang, T. Muta, H. Noguchi, X. Wang, M. Zhou, M. Yoshio, J. Power Sources 117 (2003) 137.
[39] L. Zhang, X. Wang, H. Noguchi, M. Yoshio, K. Takada, T. Sasaki, Electrochim. Acta 49 (2004) 3305.
[40] H. Kurimoto, K. suzuoka, T. Murakami, Y. Xia, H. Nakamura, M. Yoshio, J. Electrochem. Soc. 142 (1995) 2178.

[41] T.H. Cho, S.M. Park, M. Yoshio, T. Hirai, Y. Hideshima, J. Power Sources 142 (2005) 306.
[42] Y.-S. Hong, Y.J. Park, K.S. Ryu, S.H. Chang, Solid State Ioncis 176 (2005) 1035.
[43] P. Strobel, B. Lambert-Andron, J. Solid State Chem. 75 (2003) 90.
[44] J.N. Reimers, J.R. Dahn, J. Electrochem. Soc. 139 (1992) 2091.
[45] J.N. Reimers, J.R. Dahn, U. voN Sacken, J. Electrochem. Soc. 140 (1993) 2752.